Pharmaceutical Research
https://doi.org/10.1007/s11095-024-03794-z

ORIGINAL RESEARCH ARTICLE

# Development and *In-Vitro* Evaluation of Doxorubicin-Loaded Methacrylate Gelatin (GelMa)-Acrylamide Hydrogels for the Treatment of Malignant Pleural Mesothelioma

**Nishant S. Kulkarni[1] · Gautam Chauhan[1] · Mural Quadros[1] · Dnyandev G. Gadhave[1] · Vivek Gupta[1,2]**

Received: 17 June 2024 / Accepted: 8 November 2024


## Abstract

**Objective** Malignant pleural mesothelioma (MPM) is the most prevalent subtype of malignant mesothelioma that affects the pleural lining of the lungs. Conventionally, chemotherapy via systemic injections has shown limited efficacy due to off-target effects, and inefficacious deposition at the disease site. In our previous study, we reported the development and optimization of UV-initiated methacrylate gelatin (GelMa)-acrylamide based hydrogel formulation for local intracavitary administration of therapies. The current study utilizes a pre-established GelMa formulation for delivering a small molecule chemotherapeutic agent, Doxorubicin (Dox), against *in-vitro* MPM models.

**Methods** Dox-loaded hydrogel (DLH) precursor solution was prepared by dissolving Dox in the precursor solution. The gels were characterized for physical properties such as gelling time, swelling index, bio adhesion, and injectability and were compared to blank hydrogels. Dox-loaded hydrogels were also tested for therapeutic efficacy in MPM cells in various 2D and 3D cell culture models.

**Results** It was revealed that Dox-loaded hydrogels retained similar physical properties, including gelling time (< 25 s), swelling index (~ 1,200%), bio-adhesion (> 20 g detachment force), and injectability (< 2N force for injecting precursor), compared to blank hydrogels. Moreover, the gel formulation effectively sustained the release of hydrophilic Dox HCl over a period of 12 days by increasing the degree of crosslinking between GelMa and its crosslinkers. Further, the therapeutic efficacy of Dox was retained even after loading into hydrogels, indicating that no chemical interactions took place between gel excipients and the drug. Studies in MPM cell-based models revealed that DLH showed excellent potential in inhibiting 2D and 3D cell growth, with DLH being more effective than plain Dox in suppressing tumor growth in 3D spheroid models.

**Conclusions** Overall, the results of the present study suggest that Dox-loaded hydrogels (DLH) may be a good candidate for efficacy study in preclinical mesothelioma models, with strong potential for clinical translation.

**Keywords** doxorubicin hydrochloride · hydrogel · intracavitary · local delivery · malignant pleural mesothelioma · methacrylate gelatin (GelMa)

## Introduction

Malignant Pleural Mesothelioma (MPM) is one of the most common types of mesothelioma that, till date, haunts about 3,000 patients in the USA, annually [1]. Statistically, MPM is an extremely rare disease, however, it is the most fatal among all types of cancers, exhibiting the lowest 5-year patient survival, with < 10% patients surviving beyond five years of diagnosis [2]. This high patient fatality may be attributed to the high latency period between exposure to MPM causative agents and development of symptoms [3]. This latency ranges between 20- to 50-years and is usually

✉ Vivek Gupta
guptav@stjohns.edu

[1] Department of Pharmaceutical Sciences, College of Pharmacy and Health Sciences, St. John's University, Queens, NY 11439, USA

[2] College of Pharmacy and Health Sciences, St. John's University, 8000 Utopia Parkway, Queens, NY 11439, USA

Published online: 04 December 2024

indicative of a more aggressive form of cancer [4]. While there have been a few early-stage cases where patients were completely cured [5], to date, there is no cure for MPM [6]. This condition develops due to excessive inhalation of asbestos or asbestos-like fibers [7]. During the untimely collapse of world trade centers on 09/11, there were copious amounts of asbestos that was released from ground-zero, which was involuntarily inhaled by first-responders and surviving victims. Considering the latency period of this disease, those victims and first-responders remain at high-risk of developing MPM [8, 9]. MPM is often diagnosed at late-stage leaving surgical resection the first-choice therapy with extra pleural pneumonectomy and pleurectomy decortication being performed on patients [10]. However, surgical resection never guarantees complete tumor resection, which leads to tumor relapse in majority of the cases [11]. To avoid tumor relapse and to manage MPM prior to surgical resection, a small-molecule combinatorial therapy has been approved by the USFDA in 2004 which utilizes cisplatin and pemetrexed (Alimta®) [12]. Since then, no small-molecule therapy has been approved in the USA for MPM management. An immunotherapy involving Nivolumab, and Ipilimumab was recently repositioned and approved by USFDA for the treatment of MPM [13]. However, this therapy is plagued with systemic toxic effects, while being expensive [14]. Also, the major drawback for both small molecule and immunotherapy is their minimal improvement in patient survival with chemotherapy extending patient survival to 12–14 months and immunotherapy extending it to 18–19 months [13]. In spite of this being a great achievement, there have been multiple reports that suggest that patient-survival can be further improved by delivering therapeutically efficacious molecules locally to the pleural cavity [15]. However, till date, clinical use of local therapy has been limited to intra-operative or post-operative therapies, that too in investigative settings. Currently, the most important challenge faced is the frequency of administering local therapy to the pleural cavity without a need for recurrent invasive procedures. Theoretically, a delivery system can be designed that can deliver therapeutic payloads locally over a sustained period, while residing in the pleural cavity.

The most important parameters that need to be addressed while developing a localized delivery system include biocompatibility, residence time in the pleural cavity and the release profile of therapeutic payloads. One such delivery system that can address all these parameters is hydrogels, which is a 3D crosslinked network of hydrophilic polymers [16]. Crosslinking of polymers to form hydrogels can be initiated via multiple stimuli such as temperature, pH, or photo-crosslinking [17–20]. For instance, pluronic F127 is a widely used thermosensitive polymer that undergoes sol–gel transition at elevated temperatures [20]. Moreover, certain PEGylated aldehydes such as PEG benzaldehyde, when combined with chitosan can form a pH sensitive gel that can expand or shrink based on the pH [17]. This can help control the release of therapeutic payloads. Such systems are widely used in tissue engineering applications, however, apart from their application in tissue engineering and wound healing, hydrogels have been recently repositioned to be used as effective drug delivery systems [21]. This repositioning can be attributed to its ability to delay drug release and sustain it over a period of 10 days. Apart from this, versatility in the excipients that can be used to formulate hydrogels renders a wide range of physicochemical properties such as mechanical strength, bio adhesion, biocompatibility, elasticity, etc. One such widely used material is methacrylate gelatin (GelMa), a semi-synthetic polymer derived from gelatin [22]. Methacryloyl substitution on gelatin imparts photo-crosslinking ability to gelatin which can be exploited to form gels using an external stimulus such as a UV source [22]. This property allows GelMa to form covalent crosslinks with certain photo-initiators such as Irgacure 2959 or lithium acylphosphinate salts [23]. Photo-crosslinking not only aids gel formation but also improves the mechanical strength of gelatin, which is an essential trait to possess for a delivery system that is intended to reside in the dynamic environment of the pleural cavity [24]. Apart from the mechanical strength, hydrogels fabricated using GelMa also have intrinsic bio-adhesive properties, which can be attributed to the presence of cell and tissue binding arginine-glycine-aspartic acid motifs present within GelMa [22]. Over time, GelMa hydrogels are prone to enzymatic degradation by enzymes such as matrix metalloproteinases (MMP) which cleave certain amino acid residues within GelMa [25]. This biodegradability of GelMa makes it an excellent choice for local delivery to the pleural cavity as the pleural fluid is rich in MMP enzymes [26]. Local delivery to the pleural cavity can be achieved by injecting a precursor solution of GelMa hydrogels followed by provision of external UV stimulus to set the gel in place. This hydrophilic precursor solution will comprise of the polymeric backbone, crosslinkers and active therapeutic payload. GelMa hydrogels can be curated to carry hydrophobic and hydrophilic therapeutic payloads. However, due to the intrinsic hydrophilicity of hydrogels, use of hydrophilic payloads is encouraged as the loading process is straightforward and yields homogenous systems readily.

One such heavily tested hydrophilic chemotherapeutic agent is Doxorubicin Hydrochloride (DOX). DOX, an anthracycline derivative, was approved by the USFDA in 1995 for the treatment multiple cancers such as breast cancer, lung cancer, ovarian cancer, etc. [27]. DOX has an intrinsic water solubility of > 10 mg/ml making it a suitable candidate for incorporation with hydrogels [28]. Moreover, DOX has been extensively tested for its therapeutic effect against MPM and has been administered as an infusion in

combination with platinum-based molecules such as cisplatin [29]. In 2019, DOX was administered as a hyperthermic intrathoracic chemoperfusion along with cisplatin for a post-operative local treatment of MPM [30]. The local delivery of chemotherapeutics has been widely reported to improve the therapeutic outcomes in patients with MPM with a multiple-fold increase in the patient survival [31]. The use of hydrogels as a localized sustained release delivery system will yield these enhanced therapeutic outcomes without a need for frequent invasive procedures and thus improve patient compliance and increase the ease of therapy.

With this in mind, this study focuses on developing a hydrogel-based delivery system capable of local delivery to the pleural cavity using GelMa, lithium acylphosphinate salts and a chemical cross linker (NN-methylenebisacrylamide) along with DOX. Development and optimization of hydrogels was previously reported in a study that elaborated on the development for hydrogel formulations using a design of experiment approach. Extensive physical characterization was performed to ascertain the formulation composition. This study leverages the formulation that was developed in our previous report to demonstrate the therapeutic benefits of DOX-loaded hydrogels against MPM. Extensive *in-vitro* testing to validate the physical properties of drug loaded hydrogels is being reported. Moreover, this study dwells into the therapeutic testing of DOX-loaded hydrogels in 2D- and 3D-cell based MPM models. To our knowledge, this is the first study describing intracavitary applications of GelMa based hydrogels for malignant mesothelioma treatment.

## Materials

Photogel® Methacrylated Gelatin (GelMa) was purchased from Advanced Biomatrix inc. (Carlsbad, CA, USA). Lithium phenyl-2,4,6-trimethylbenzoylphosphinate (LAP), the photoinitiator used to crosslink with GelMa, was procured from Sigma-Aldrich (St. Louis, MO, USA). A chemical crosslinker, NN-methylenebisacrylamide (BIS), was procured from Acros Organics B.V.B.A (Geel, Belgium). Doxorubicin Hydrochloride salt was procured from LC Labs (Woburn, MA, USA). A UV source with an intensity of 760 μwatts/cm$^2$ was procured from Analytik Jena (Upland, CA, USA). Guinea Pig lungs for bio adhesion studies were procured as frozen samples from Lampire Biological Laboratories Inc. (Pipersville, PA, USA). MSTO-211H and H226 cells were used to assess toxicity of fabricated dox-loaded hydrogels and were procured from ATCC (Manassas, VA, USA). Cell titer blue and Lactate Dehydrogenase (LDH)-Glo™ cytotoxicity assay kits were procured from Promega Corporation (Madison, WI, USA). Live/dead cytotoxicity assay kit which was used to study the viability of mesothelioma cells, was procured from Biotium Inc. (Fremont, CA, USA). Other reagents were of analytical grade, and were purchased from various third-party vendors.

## Methods

### Drug-Excipient Compatibility Studies

To evaluate the compatibility of various hydrogel components and DOX, we performed extensive drug-excipient compatibility studies by using UV spectroscopy, FT-IR, and UPLC based assessment. The detailed methods for these studies are provided in Supplementary Information.

### Fabrication of Hydrogel Precursor Solution (PS)

Hydrogel precursor solution (PS) was formed by solubilizing DOX (0.1 mg), GelMa (5% w/v), LAP (0.5% w/v) and BIS (2.5% w/v) in phosphate buffer saline to yield a Dox-loaded hydrogel precursor solution (DLH-PS). The concentrations and rationale for each hydrogel component was previously established in our published study [32]. Briefly, a design of experiment approach was undertaken by designing a $2^3$ factorial design. Multiple formulations were developed in-house and subjected to rigorous physical characterization. Gelling time was the defining factor for attrition of multiple formulations. Bio adhesion led to the attrition of the formulations further help attain the optimized formulations for GelMa hydrogels with GelMa (5% w/v), LAP (0.5% w/v) and BIS (2.5% w/v). Further, this formulation was subjected to bath sonication at 37°C for 30 min followed by overnight shaking at 180 rpm. The precursor solution was stored at 4°C.

### Physical Characterization of Dox-Loaded Hydrogels (DLH)

DLH was physically characterized for its gelling time, injectability, bio-adhesion, swelling index, elasticity (tensile strength), and scanning electron microscopy. These characterizations were completed as per our previously reported study [32]. Detailed methods can be found in the Supplementary Information of this manuscript.

### Effect of Gelling time on *In-Vitro* Release

As previously established, increasing the UV exposure time on hydrogel PS increases the degree of crosslinking, leading to a minimization of burst release of small molecules [32]. To assess the extent of release of DOX from DLH and to ascertain the gelling time for DLH which would yield the desired DOX release profile, release of

DOX from DLH was analyzed when hydrogels were gelled at their original gelling time (25 s.), two times the gelling time (2x, 50 s.) and four times the gelling time (4x, 100 s.). 1 mL of 1X PBS was used as the release medium and released DOX was analyzed by evaluating the fluorescence intensity (565 ex/595 em) using a plate reader (Tecan, Mannedorf, Switzerland).

### *In-Vitro* Release

To determine the drug release profile of DOX from DLH, *an in-vitro* release study was designed using 1X PBS as the release media, following the protocol established earlier. Briefly, 100 µg of DOX was loaded onto 0.3 ml of hydrogel PSs. DLH-PS was gelled and placed in a 60 mm petri dish along with 1 ml of 1X PBS solution. Release media was completely replenished at every time point and the amount of DOX released from DLH was analyzed by evaluating the fluorescence intensity (565 ex/595 em) on a plate reader (Spark 10 M, Tecan, Mannedorf, Switzerland). DOX release from DLH was tested on release kinetic models (Zero order, First order, Higuchi model, Hixson-Crowell model, and Korsmeyer-Peppas model) to predict the order of drug release.

### Precursor Solution Accelerated Stability Studies

To assess the stability and performance of DLH-PS after being exposed to long term storage conditions, an accelerated stability study was designed. Briefly, DLH-PS was stored at 40°C/75% RH for four weeks. Gelling time and DOX entrapment were analyzed prior and after the four-week storage. Gelling time was evaluated as previously mentioned, while DOX entrapment was evaluated by measuring the fluorescence intensity (565 ex/ 595 em) using a plate reader (Tecan, Mannedorf, Switzerland).

### Therapeutic Testing

#### Cell Lines and Culture Conditions

In this study, MSTO-211H and H226 immortalized malignant mesothelioma cell lines were procured from American Type Culture Collection (ATCC, Manassas, VA, USA); and were used to perform *in-vitro* efficacy testing. Both cell lines were cultured using RPMI-1640 cell growth medium supplemented with 10% Fetal Bovine Serum, 1% sodium pyruvate and 1% penicillin–streptomycin. The cells were grown at 37 °C/5% $CO_2$ in tissue culture (TC) treated T75 cell culture flasks (Eppendorf, Hauppauge, NY, USA) until 80–85% confluency was reached. Confluent cells were trypsinized and used for *in-vitro* experiments.

#### Determination of $IC_{50}$ Value for DOX in MPM Cells

To determine the $IC_{50}$ value for DOX in MPM cells, MSTO-211H and H226 immortalized MPM cell lines were used. Briefly, cells were cultured as described in the previous section followed by seeding in sterile TC-treated 96-well plates at a density of 2,500 cells/well. Cells were incubated overnight at 37 °C/5% $CO_2$ to facilitate adherence. The following day, cells were treated with varying concentrations of DOX (9-nM to 10-µM) and incubated further for 48 h. Cell viability was evaluated using Cell titer® Blue cell viability assay kit (Promega Corporation, Madison, WI, USA) by following manufacturer's protocol. Briefly, after 48 h of treatment, 20µL of cell-titer blue reagent was added to the cells without aspirating the treatments. Cells were then incubated at 37 °C/5% $CO_2$ for two hours followed by a measurement of fluorescence. Cell viability was calculated relative to control. $IC_{50}$ values for DOX in both cell lines was calculated using GraphPad Prism software (GraphPad Software, San Diego, CA, USA). All cell viability assays were performed in duplicates with $n = 6$ each time.

#### Live/Dead Assay

To evaluate the therapeutic efficacy of DLH, a live/dead cell assay was designed. Briefly, a live/dead assay was performed using MSTO-211H cells. Cells were seeded in a TC-treated 24-well plate at a density of 40,000 cells/well. Following overnight incubation at 37 °C/5% $CO_2$ to facilitate adherence, cells were treated with DOX (0.15- and 0.39- µM) and DLH (0.39- and 0.78-µM) for a period of 48 h. DLH was made by exposing DLH-PS to UV light (365 nm) while maintaining sterile conditions. Hydrogels were then carefully placed inside the 24-well plates such that adhered cells were in contact with the gels. This strategy was adopted to simulate the potential intrapleural interaction between the cells of the pleural lining and adhered hydrogels as reported earlier [32]. After that, live and dead cells were stained using Live/dead viability/cytotoxicity assay kit (Biotium, Fremont, CA, USA), following manufacturer's protocol. Briefly, treatments were aspirated after the set time point followed by addition of sterile phosphate buffer saline spiked with calcein AM and ethidium homodimer III dyes. Cells were stained for 30 min at room temperature. Live cells were stained using calcein AM and dead cells were stained using ethidium homodimer III (EthD-III). Cells were imaged using an Evos FL fluorescence microscope (4 × objective) (Thermo Fisher Scientific, Waltham, MA, USA) using GFP (green fluorescence protein for calcein AM) and RFP (red fluorescence protein EthD-III) filters respectively.

### 3D Spheroid Models

3D cell-based tumor spheroids were developed for MSTO-211H cells using PrimeSurface® 3D culture Ultra-low Attachment 24 well flat bottom plate (S-bio, Hudson, NH, USA). Briefly, 20,000 cells/well were seeded in 24-well plates and were incubated at 37 °C/5% $CO_2$ conditions for three days to yield robust tumor masses. After three days, tumor masses were treated with varying concentrations of DOX (0.15- and 0.39-µM) and DLH (0.39- and 0.78-µM) for a period of six days. DLH was made by exposing DLH-PS to UV light (365 nm) while maintaining sterile conditions. Hydrogels were then carefully placed inside the 24-well plates such that adhered cells were in contact with the gels. This strategy was adopted to simulate the potential intrapleural interaction between the cells of the pleural lining and adhered hydrogels as reported earlier [32]. 3D-tumor masses were imaged using Evos FL fluorescence microscope (4 × objective) (Thermo Fisher Scientific, Waltham, MA, USA) using the transmittance filter after treatments on day one, three and six; and images were subjected to evaluation of tumor mass area using ImageJ software. Media replenishment was done on day 3 when tumor masses were supplied with a fresh nutrient media.

### LDH-Glo Cytotoxicity Assay

To evaluate the therapeutic efficacy of DOX and DLH in tumor spheroids, an LDH-Glo cytotoxicity assay was carried out to assess the lactate dehydrogenase content in the nutrient media that housed tumor masses. Briefly, cell culture media samples were collected three days after treatment with DOX (0.15- and 0.39- µM) and DLH (0.39- and 0.78- µM), analyzed for their LDH levels using LDH-Glo™ cytotoxicity assay kit (Promega corporation, Madison, WI, USA) following manufacturer's protocol. Cell culture media samples were diluted using a storage buffer comprised of Tris–HCL (200 mM, pH 7.3), glycerol (10%) and BSA (1%) at specific concentrations. Diluted media samples were further incubated with LDH detection mix and reductase substrate enzyme for 30 min followed by recording luminescence signals using a Tecan plate reader (Mannedorf, Switzerland).

## Statistical Analysis and Data Presentation

All data presented here are mean ± SD or SEM ($n = 3–6$). Unpaired student's t-test was used to compare two groups whereas to compare more than two groups, one-way ANOVA followed by Tukey's post hoc multiple comparison test was used. $p < 0.05$ *or less* was considered statistically significant and is reported throughout the manuscript.

# Results

## Drug-Excipient Compatibility Studies

### FT-IR

To mimic formulation conditions, DLH-PS and blank hydrogel PS were formulated followed by lyophilization to remove all water. Lyophilized formulations were subject to FT-IR analysis to qualitatively determine the presence of DOX in a stable form, i.e., free of chemical interactions with hydrogel components. Figure 1A represents the IR spectra for pure DOX, lyophilized blank hydrogel-PS and DLH-PS. As can be seen that DOX showed characteristic peaks at 1731 $cm^{-1}$ (Carbonyl stretching) and 3313 $cm^{-1}$ (Amine stretching.) PS without DOX also exhibited peaks at similar wavenumber, indicating an overlap of carbonyl and amine stretching from the hydrogel components. Due to these overlapping peaks, it is difficult to qualitatively determine the presence of DOX in a stable form.

### UV-Based Assessment of DOX Stability

A UV spectrophotometry study was designed to evaluate the compatibility of DOX with hydrogel components in a liquid state without the need for lyophilization. Figure 1B shows that DOX had an absorbance peak at 488 nm wavelength, while no other hydrogel component exhibited an absorbance peak at that wavelength. Further, DOX was solubilized along with GelMa, LAP and BIS as separate mixtures at the ratio representative of the final DLH formulations. Moreover, absorbance scan of DLH-PS and DLH was also performed to understand the compatibility of DOX in the final formulation. Figure 1B revealed the characteristic DOX absorbance peak at 488 nm in all liquid mixtures including DLH-PS and DLH. This indicated that DOX is present in a stable form inside the formulations and is compatible with all hydrogel components.

### UPLC Analysis to Assess Dox Degradation

To further establish the compatibility of DOX with all hydrogel components, DOX in its free form and in DLH-PS was analyzed using UPLC. As seen in Fig. 1C, DOX has a retention time of 1.055 min when analyzed using a reversed phase C18 column at 234 nm wavelength (as described in *Methods*). Whereas, when injected as DLH-PS, DOX peak slightly shifts to 1.135 min (Fig. 1D), while exhibiting excipient peaks that belong to GelMa, LAP and

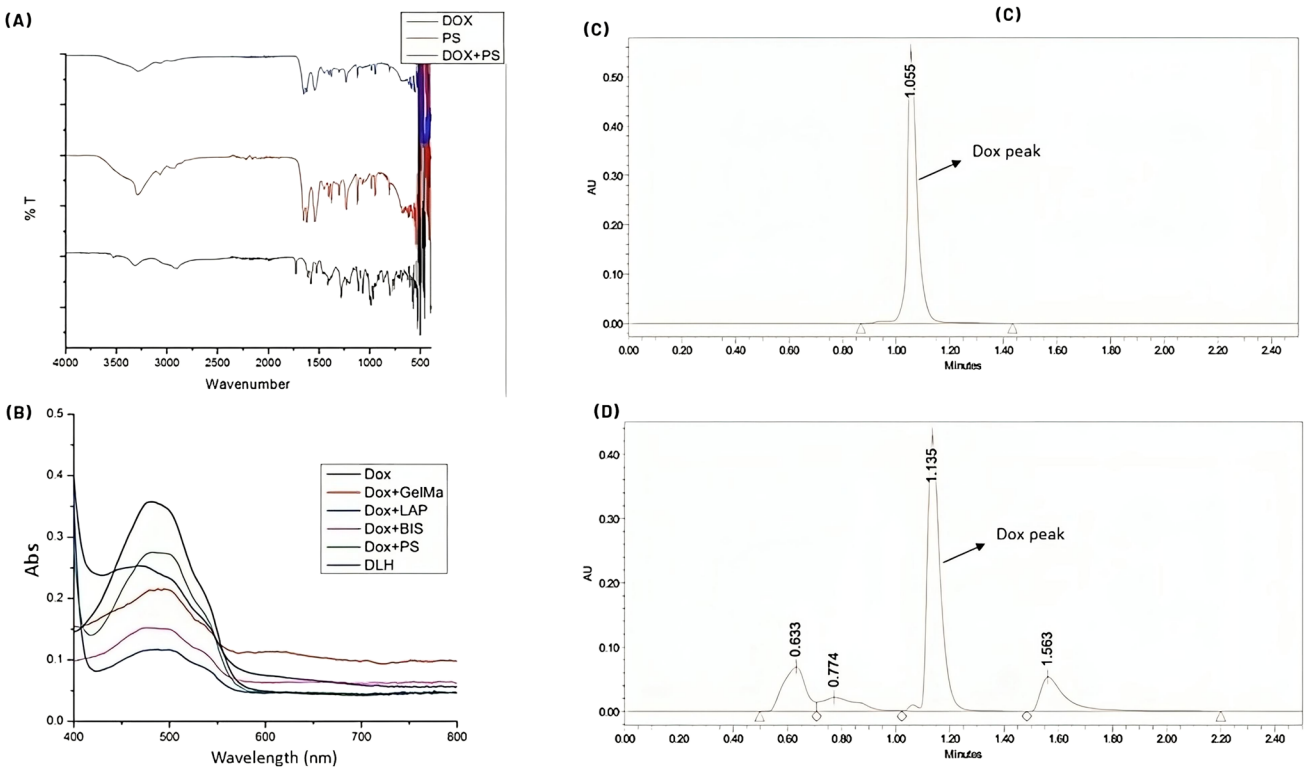


**Fig. 1** (**A**) FTIR analysis spectra representing DOX, blank precursor solution and DLH-PS. (**B**) Plots represent UV absorption peaks for hydrogel components and DOX. UV analysis was done for DOX solubilized along with excipients, DLH-PS, and DLH. (**C**) Chromatograms represent standard DOX peak in comparison with peak for (**D**) DOX extracted from DLH. All data represents $n = 3$ (mean ± SD).

BIS. However, no degradation in DOX peak was observed when injected as DLH-PS, indicating excellent compatibility between DOX and all hydrogel components. This study further confirmed that DOX exhibits good compatibility with GelMa, LAP or BIS.

## Physical Characterization of Dox-loaded Hydrogels (DLH)

For a complete therapeutic evaluation of the previously established formulation, DOX was loaded into optimized hydrogels and tested against *in-vitro* models of malignant pleural mesothelioma. Loading cargo into pre-established hydrogels may lead to alterations in certain physical properties for hydrogels. This alteration may be attributed to the interference of the loaded cargo with crosslinking of the polymeric backbone and crosslinkers, leading to a diminished or amplified degree of crosslinking [33]. This change in crosslinking can either negatively or positively affect previously established physical properties of the optimized hydrogels. In an ideal scenario, any cargo that is loaded into the hydrogels should be inert and should not significantly change the physicochemical properties of the gels.

### Gelling Time

This study was designed to ascertain that loading DOX into hydrogels does not affect the time required for a complete sol–gel conversion, as DOX does not interact with any hydrogel component, as confirmed via drug-excipient compatibility studies (Fig. 1). In this study, the gelling time for DLH was found to be 23.7 ± 2.9 s whereas blank hydrogel was 26.2 ± 7.6 s (Fig. 2A). This difference in gelling time pre- and post-DOX loading was found to be statistically insignificant, indicating no change in gelling time post-DOX loading.

### Injectability

This study was carried out to understand the effect of DOX loading on the ability of DLH-PS to be injected through a 26-gauge needle. A 26-gauge needle (internal diameter of 0.26 mm) was selected to mimic the potential route of administration of the optimized hydrogel formulations which is through a catheter tubing that accesses the pleural cavity in MPM patients, and has an average internal diameter of 0.3 mm. The force required to inject hydrogel PS may be affected due to DOX loading if DOX loading is enhancing the viscosity of the pre-established hydrogel PS. It was

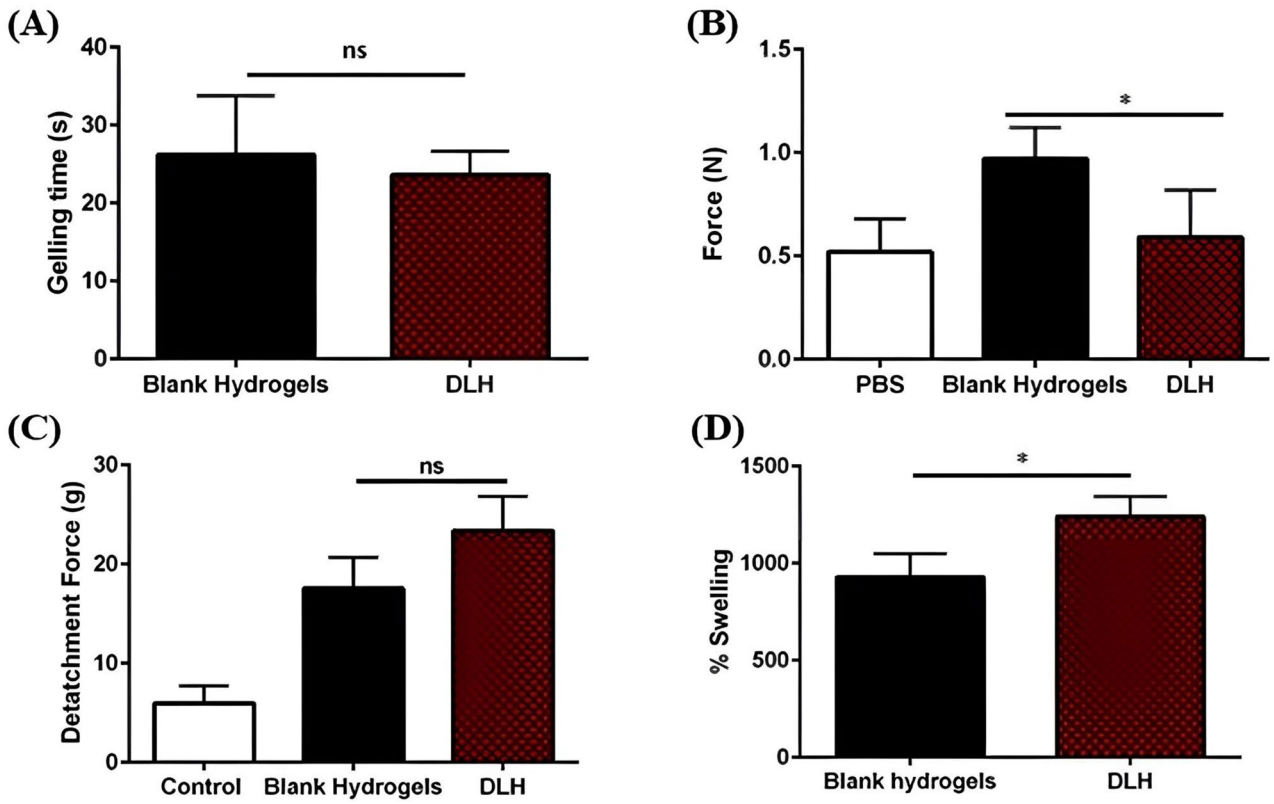


**Fig. 2** (**A**) Plot represents gelling time analysis for blank hydrogels and DOX-loaded hydrogels. (**B**) Plot represents the force required to inject blank hydrogel PS and DLH-PS relative to the force required to inject 1X PBS. (**C**) Plot represents the force required to detach blank hydrogels and DLH from guinea pig lung tissues. (**D**) Plot represents swelling index for blank hydrogels and DLH. All data represents $n=3$ (mean ± SD). *(*$p<0.05$).*

revealed that DLH-PS required a force of 0.59 ± 0.23 N to be injected through the 26-gauge needle, which was minutely statistically significant ($p=0.0473$) to the force required to inject hydrogel PS without DOX (1.0 ± 0.1 N). However, the difference is insignificant as compared to a solution of 1X PBS (0.52 ± 0.16 N) (Fig. 2B). This study confirmed that DLH-PS can still be injected through a catheter tube for local delivery of DOX to the pleural cavity.

### Bio-Adhesion

Bio-adhesion of hydrogels depends on the degree of crosslinking between the polymeric backbone and crosslinkers. This degree of crosslinking may be affected after loading cargo such as DOX in hydrogels. So, to assess the effect of DOX loading on bio-adhesion, the force of detachment of blank hydrogels and DLH from activated guinea pig lung tissues was evaluated using a texture analyzer (TA_XT Plus). This experiment revealed that there was no significant difference in the force required to detach blank hydrogels (17.55 ± 3.15 g) and DLH (23.37 ± 3.45 g) *($p=0.0971$)* (Fig. 2C). However, both hydrogel formulations required significantly higher force to detach as compared to a reference solution 1X PBS (5.97 ± 1.77 g), indicating the degree of bio-adhesion for the fabricated hydrogel. Therefore, this study confirmed that DOX loading did not affect the intrinsic bio-adhesion properties of the optimized blank hydrogel.

### Swelling Index

This study was designed to assess the effect that DOX may have on the swelling index of hydrogels by interfering with the degree of crosslinking between GelMa, LAP and BIS. The swelling index for blank hydrogel was found to be 928.8 ± 119.7% whereas for DLH it was 1238.9 ± 104.5% ($p=0.0278$) (Fig. 2D). It can be concluded that DLH loaded hydrogels tend to swell more as compared to blank hydrogels. A higher degree of swelling should be ideal for a sustained release of DOX from hydrogels.

### Tensile Strength Measurement

Hydrogels designed to live in physiological cavities may withstand dynamic environments such as fluid exchange in the peritoneal cavity, lung inflation and deflation in the pleural cavity, etc. Therefore, it is critical to assess the hydrogel's

elasticity. Elasticity for blank and DOX-loaded hydrogel (DLH) was evaluated using TA.XT Plus texture analyzer, by measuring the force required to puncture hydrogels with respect to the distance traveled by the probe (Fig. S1). Values of Young's modulus (MPa) was then calculated to ascertain the degree of elasticity. Young's modulus for the blank and DLH was computed to be $7.5 \pm 0.8 \times 10^{-4}$ MPa and $7.79 \pm 1.9 \times 10^{-4}$ MPa, respectively. Both values were found to be extremely low (< 0.1), suggesting that all formulations are very elastic and would not impede the functioning of the organ located in the cavity of interest. Moreover, no significant difference in Young's Modulus was observed between blank and DLH.

### Scanning Electron Microscopy

Morphological analysis of blank hydrogels and DLH exhibited a macroporous structure which reaffirmed that hydrogel swelling was not affected by DOX loading (Fig. 3). Retention of the macroporous structure also suggested that other physical characteristics of hydrogels, such as mechanical strength or elasticity, which depend on the existence of macropores, may not be impacted by DOX loading. Moreover, Fig. 3 showed that DOX crystals were found encircling the matrix hydrogel structure after freeze drying.

### Effect of Gelling Time on *In-Vitro* Release

It was previously established that increasing gelling time beyond the minimum time that is required to gel hydrogels using LAP and BIS can curb the extent of burst release for hydrophilic small molecules [32]. This phenomenon was tested to evaluate the extent of burst release of DOX from DLH to curate the sustained release of DOX over a period of 2- and 4-h. Figure 4A revealed that in 2 h, 25 s of gelling resulted in a DOX release of $37.1 \pm 3.1\%$ whereas by increasing the gelling time by 2× and 4x, DOX release in the first two hours was significantly delayed to $24.0 \pm 4.5\%$

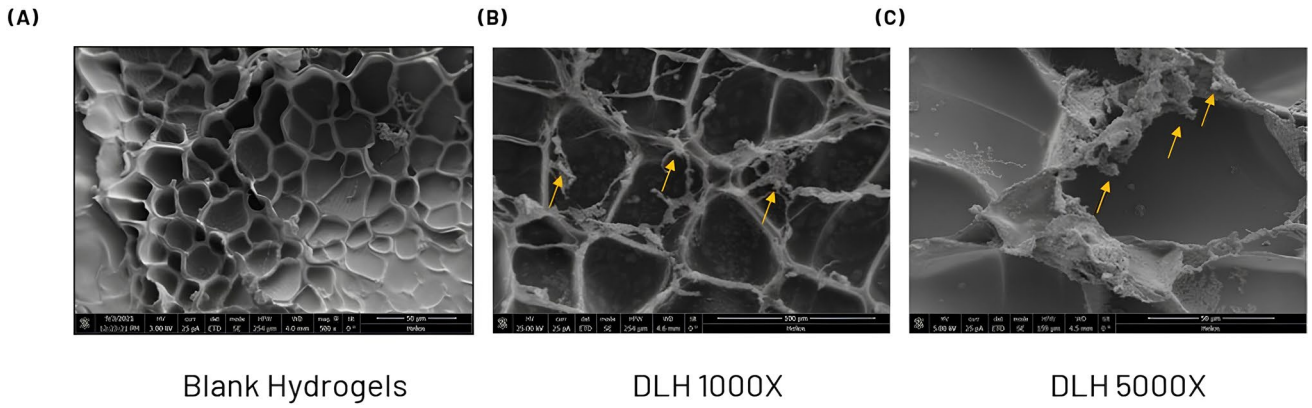


**Fig. 3** (**A**) Micrographs represent the mesh-like hydrophilic polymeric network within hydrogels without Dox loading (500x). (**B**) & (**C**) Dox-loaded hydrogels were lyophilized followed by sectioning and loading on SEM-compatible stubs. Micrographs reveal DOX crystals around the hydrophilic polymeric matrix structure within hydrogels. (**B**) represents micrographs at 1000× and (**C**) represents micrographs at 5000×.

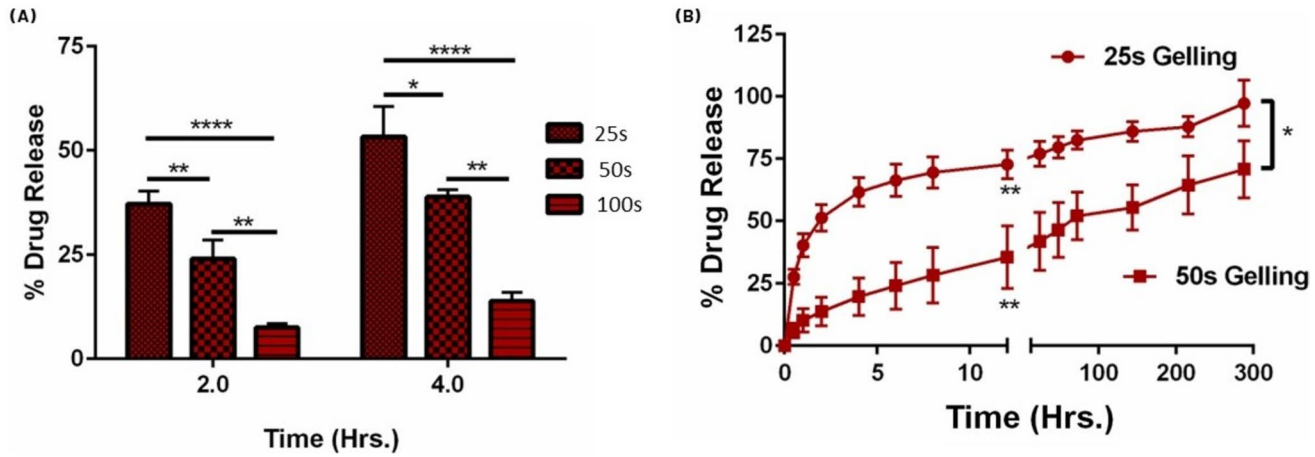


**Fig. 4** (**A**) Plot represents the effect of gelling time on DOX release from DLH. (**B**) Plot represents the release profile of DOX over 12 days after 25 s and 50 s of gelling time. All data represents $n = 3$ (mean ± SD). *(*$p < 0.05$, ** $p < 0.01$, **** $p < 0.0001$)*.

($p < 0.01$) and 7.5 ± 0.9% ($p < 0.0001$), respectively relative to 25 s of gelling. A similar effect was observed within the first 4 h of DOX release where in 25 s of gelling resulted in 53.3 ± 7.3% of DOX release which was significantly more than the release after 2x (38.8 ± 1.7%, $p < 0.05$) and 4x (13.9 ± 2.1%, $p < 0.0001$) gelling times. This result indicates that it is possible to curate the burst release of hydrophilic small molecules from hydrogels, which is crucial while designing a localized sustained release delivery system.

## *In-Vitro* Release

While studying the effect of gelling time on DOX release, it was revealed that DOX has a burst release of 53.3 ± 7.3% within the first four hours. Increasing the gelling time two folds significantly reduced the burst release and thus to study the *in-vitro* release profile and kinetics of DOX from DLH, DOX release after 25 s of gelling was compared with DOX release after 50 s of gelling. A four-fold gelling of DLH (100 s) resulted in a significant delaying of DOX release, which may not be suitable to achieve the desired therapeutic response in MPM; and hence was not tested. Figure 4B represents the *in-vitro* release of DOX over 288 h (12 days) from DLH gelled for 25- and 50-s. As can be seen, DLH gelled for 25 s had an average DOX release of 40.3 ± 4.6% in the first hour while for 50 s exhibited a DOX release of 10.3 ± 4.7% in the first hour. DOX release steadily increased over a period of 12 days when DLH gelled for 25 s had a cumulative release of 97.3 ± 9.3%, which was significantly more than the cumulative release of DOX from DLH gelled for 50 s. (70.8 ± 11.4%, $p < 0.05$).

Release kinetics of DLH were assessed using numerous mathematical models, including first-order release, second-order release, Higuchi release model, and Korsmeyer-Peppas release model, utilizing data obtained from the *in vitro* release study. Among these models, Higuchi release kinetic model ($R^2 = 0.9248$ and 0.9983) demonstrated the best fit for DLH gelled for 25 s and 50 s respectively (Table I). Fig. S2 displays a linear curve for the Higuchi model compared to other models**.** This observation confirms that increasing the gelling time of DLH results in a controlled and sustained release of DOX via a diffusion mechanism due to a higher degree of crosslinking.

**Table I** The Regression Coefficient of *In-Vitro* Release Kinetic Models Observed for DLH Formulations

| Release kinetic models | Formulations | |
|---|---|---|
| | 25-sce gelling ($R^2$) | 50-s gelling ($R^2$) |
| Zero-order | 0.7213 | 0.9292 |
| First-order | 0.8554 | 0.9518 |
| Higuchi | 0.9248 | 0.9983 |
| Hixon-Crowel cube root | 0.8138 | 0.9445 |
| Korsmeyer-Peppas<br>$n$ = Release exponent | 0.6731<br>($n$ = 0.1966) | 0.8514<br>($n$ = 0.8233) |

$R^2$: Regression coefficient

## Precursor Solution Accelerated Stability Studies

To account for the storage conditions of the precursor solution, accelerated storage stability conditions were simulated for DLH-PS. The key performance factor for DLH-PS after long term storage is its ability to gel on UV exposure as well as the amount of DOX loaded into hydrogels.. Figure 5A demonstrates that the least amount of time needed for DLH-PS to gel and produce DLH was 24.5 ± 1.3 s on day 0 whereas the measured gelling time was 24.3 ± 0.52 s after

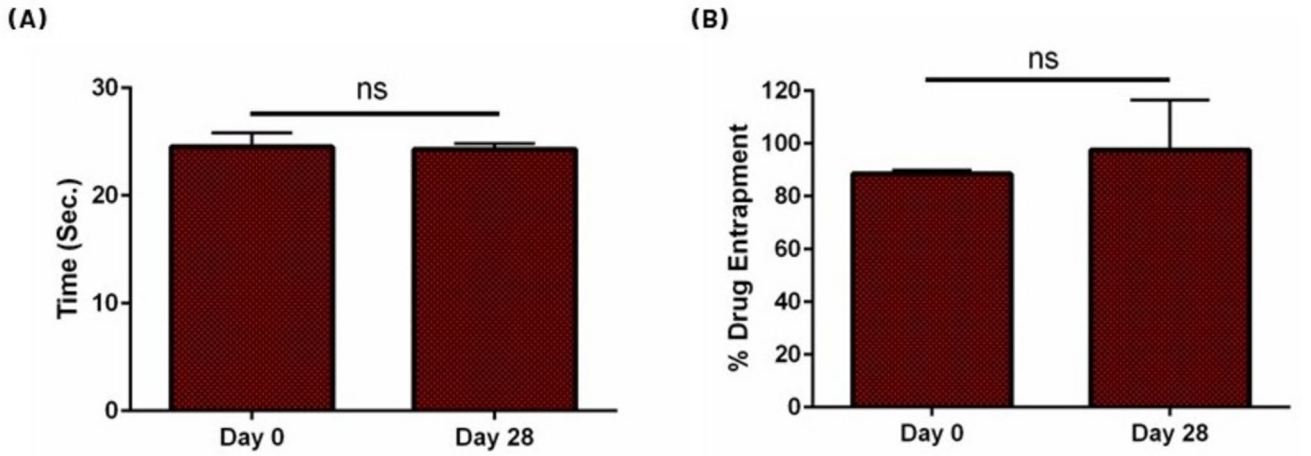


**Fig. 5** Plot represents the precursor solution stability for DLH-PS, assessed with respect to (**A**) gelling time and (**B**) DOX entrapment in DLH over a period of 28 days. Dox-loaded precursor solutions were stored at 40°C/75% RH for a period of 28 days followed by performance assessment. All data represents $n = 3$ (mean ± SD).

4 weeks of incubation (Day 28). DOX loading recorded on day 0 was found to be 88.6 ± 1.3% while after a 4-week incubation, it was 97.6 ± 19.0% and no statistical significance was observed between the DOX loading, indicating excellent precursor solution storage stability (Fig. 5B).

## Therapeutic Testing

### Determination of $IC_{50}$ Value for DOX in MPM Cells

This proof-of-concept experiment was designed to determine the $IC_{50}$ values of DOX in 2D *in-vitro* cell-based models comprising of MSTO-211H and H226 immortalized cells. These $IC_{50}$ values would further be used to test DLH efficacy in both 2D and 3D models. Preliminary cytotoxic evaluation of the potent chemotherapeutic DOX in both cell lines revealed excellent DOX efficacy in both cell lines with $IC_{50}$ values of 0.11 ± 0.02 µM (MSTO-211H) and 0.27 ± 0.01 µM (H226) (Fig. 6A). 2D and 3D therapeutic models for testing the efficacy of DLH would be designed based on the $IC_{50}$ values obtained from this study.

### Live/Dead Assay

Live/Dead cell assay was used to visualize the population of live and dead cells within untreated and treated MSTO-211H cells. A higher loading of DOX was required to test out DLH in an *in-vitro* setting to account for the sustained release of DOX from DLH. Cumulative release of DOX from DLH in 48 h was 46.49 ± 10.9211.0% and thus, an accurate comparison of DLH efficacy would be to compare the dead cell population of 0.15- and 0.39-µM DOX treated group with 0.39- and 0.78-µM DLH treated cells, respectively. In Fig. 6B, live cell population is represented by green fluorescence, whereas dead cell population is presented by red fluorescence. As shown in Fig. 6B, untreated MSTO-211H cells did not exhibit abundance of red punctate that denoted dead cells, indicating higher cellular viability after 48 h of incubation. However, cells treated with DOX and DLH, at both tested concentrations have abundant red punctate, indicating therapeutic efficacy in inhibiting MSTO-211H cell survival after a 48-h treatment period. The population of red punctate in 0.39 µM DLH treated cells was higher than 0.15 µM DOX treated cells, and this may be attributed to the higher cellular interaction of MSTO-211H cells with hydrogels due to the presence of cell-binding motifs such as the RGD sequence in the polymeric backbone (GelMa) of hydrogels (Fig. 6B). This qualitative study revealed the efficacy of both DOX and DLH in enhancing necrotic cells population in MSTO-211H cells.

### 3D Spheroid Models

At every time point (Days 0 (treatment day) 1 (24 h), 3 (72 h) and 6 (144 h)), tumor masses were imaged and analyzed for their surface area using ImageJ opensource software (Fig. 7A). It was revealed that over a period of 6 days, untreated tumor masses had a 1.7 ± 0.2-fold increase in their area as compared to their area on Day 0, whereas DOX and DLH treated spheroid either had a constant area over six days or had multiple fold reduction in their area (Fig. 7B). Accounting for the slow release of DOX over 6 days (55.3 ± 9.1%), the efficacy of DOX 0.15- and 0.39-µM directly compared to the efficacy of DLH 0.39- and 0.78-µM, respectively. DOX 0.15 µM treated tumor masses had 0.91 ± 0.16 times area relative to the day of treatment (Day 0) whereas DLH 0.39-µM treated tumor masses had a 0.67 ± 0.14 times area on day 6 relative to the area of the group on day 0 (Fig. 7B) ($n = 6$, $p = 0.0200$). Similarly, DOX 0.39 µM treated tumor masses had 1.00 ± 0.13 times area relative to the day of treatment (Day 0), whereas DLH 0.78-µM treated tumor masses had a significantly lower area

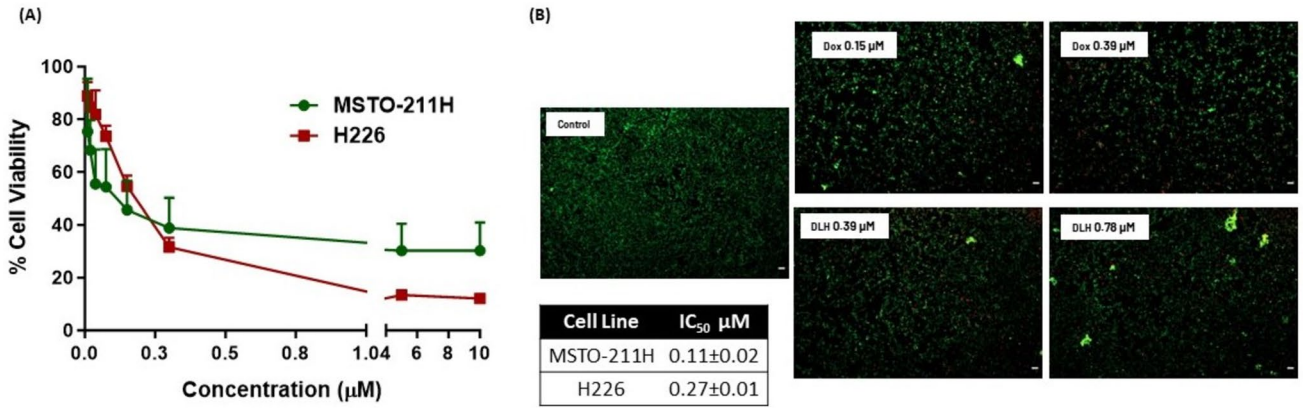


**Fig. 6** (**A**) Plot represents the % cell viability for MSTO-211H and H226 cells after DOX treatment for 48 h. Table represents the $IC_{50}$ values of DOX in both cell lines. (**B**) Images represent the live and dead cell population in MSTO-211H cells after DOX treatment for 48 h. Scale bar 50 µm. All data represents $n = 3$ (mean ± SD).

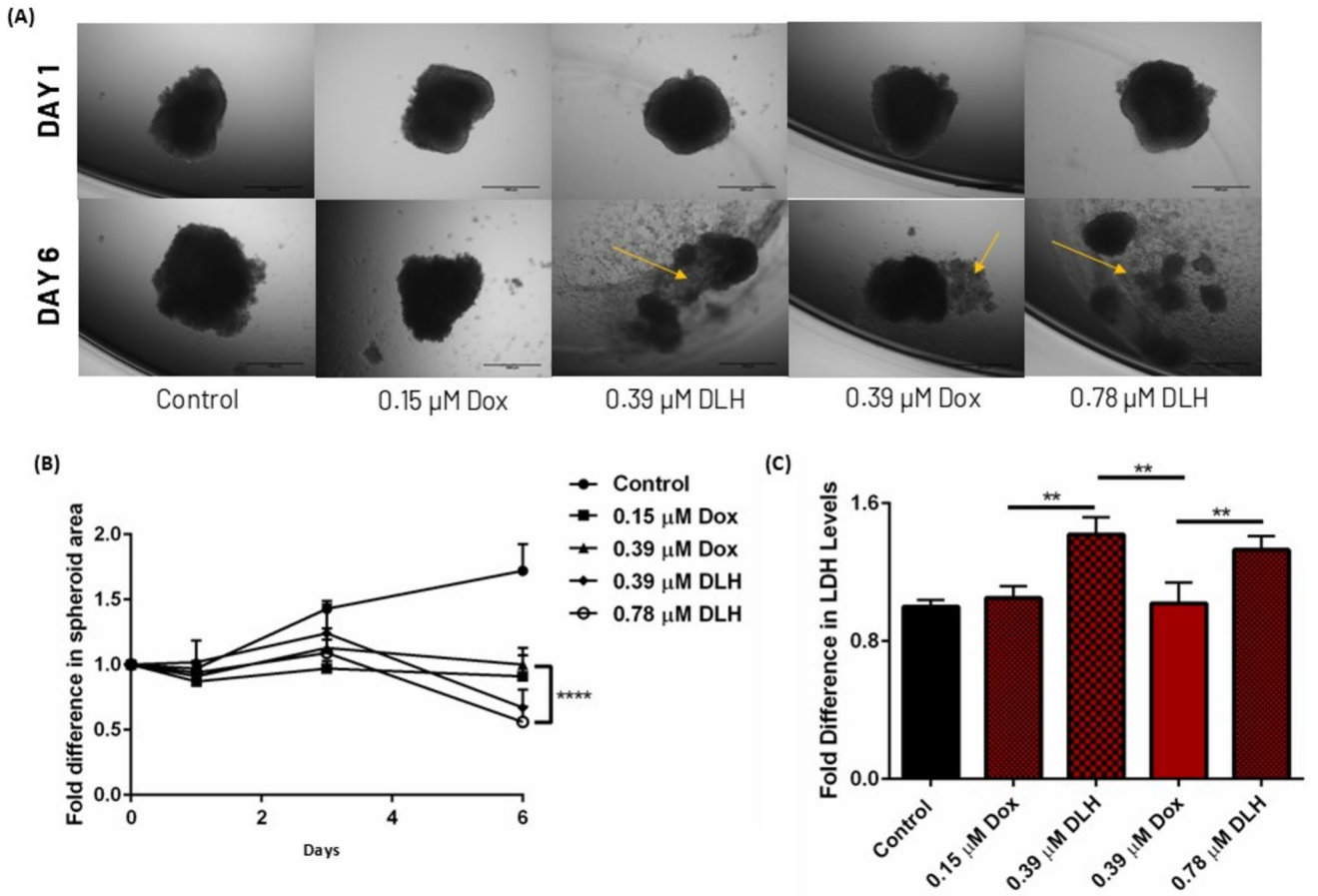


**Fig. 7** (**A**) Images represent growth of 3D tumor models comprised of MSTO-211H cells over six days with or without DOX and DLH interventions. Arrows indicate the disintegration of intact tumor masses over 6 days of treatment with free-dox or DLH (**B**) Plot represents the fold difference in the tumor mass area over 6 days. (**C**) Plot represents the fold difference in LDH levels in the nutrient media that housed treated and untreated spheroids. Scale bar 1000 μm. All data represents $n = 3$ (mean ± SD). *(** $p < 0.01$, **** $p < 0.0001$)*.

(0.56 ± 0.12) on day 6 relative to the area of the group on Day 0, $p < 0.0001$) (Fig. 7B). Along with the availability of released DOX inside the well plate, a higher therapeutic effect of DLH in 3D MPM models may also be attributed to the presence of cellular binding motifs in GelMa that promote tumor cells binding with hydrogel which exposes tumors to DOX within the hydrogel.

### LDH-Glo Cytotoxicity Assay

LDH levels were evaluated on day 3 since fresh nutrient media was supplied to tumor masses on day 3 to provide nourishment for tumor growth. It was revealed that relative to the LDH levels in nutrient medium of untreated tumor masses, DOX 0.15 μM treated tumor mass medium had 1.05 ± 0.07-fold higher LDH levels whereas DLH 0.39 μM treated tumor mass medium had 1.42 ± 0.10-fold significant higher ($p < 0.01$) LDH levels than untreated cells. Similar enhancement in LDH levels were observed for DLH 0.78 μM (1.33 ± 0.08-fold, $p < 0.01$) treated nutrient medium which was significantly higher than LDH level amplification in DOX 0.39 μM (1.02 ± 0.12 fold) treated nutrient medium (Fig. 7C). Higher levels of LDH in nutrient media treated with DLH indicates higher therapeutic efficacy in disrupting the cell membrane of cells that make up the robust 3D tumor mass which can be correlated to higher efficacy against MPM tumor masses.

## Discussion

Malignant Pleural Mesothelioma (MPM) is an incurable disease that is caused almost exclusively due to the inhalation of asbestos [34]. MPM has been reported to have the lowest patient survival [2] with conventional chemotherapeutic infusion of potent chemotherapeutics improving the patient survival marginally. There has been a rise in strategies to improve patient survival and immunotherapeutic interventions are now approved for the treatment of MPM. However, these therapies are plagued with systemic side effects, limiting their extensive use.

With an aim to provide therapeutic alternatives for MPM management, developability assessment of hydrogels was investigated in this study. Multiple pre-operative and post-operative hydrogel based therapies have been developed pre-clinically and have been reported with minimum to no clinical translation [35]. With an aim to provide an efficient and scalable platform, Dox loaded GelMa hydrogels have been developed and evaluated as part of this study. Critical quality attributes (CQA) such as high bio adhesion and biocompatibility were heavily investigated. Along with these CQAs, sustained release capabilities of delivering Dox over a few days was investigated. The listed CQAs along with a sustained delivery of therapeutic payloads may result in improved patient compliance and this can be attributed to a reduction in invasive procedures and reduced dosing frequency. Moreover, local delivery will ameliorate toxic off-target effects of potent chemotherapeutics. GelMa hydrogels have been previously reported to be bio adhesive [32] and, in this study, it was ascertained that loading Dox does not compromise the adhesive properties of the system. Moreover, GelMa, BIS and LAP have all been reported to be biocompatible [36] and this was further confirmed by the biocompatibility studies performed in the previously reported development study in 2023 [32].

Along with these CQAs, physical characterization of DOX-loaded hydrogels (DLH) evaluated in this report shed light on potential alterations in hydrogel properties in presence of a potent chemotherapeutic. Gelling time, a critical parameter for therapeutic applications, showed no significant change post-DOX loading. However, minor decrease in injectability force and an increase in the degree of swelling that was observed is in harmony with findings from studies exploring the impact of drug loading on hydrogel [33]. The difference in injectability force can be attributed to the hydrophilic interaction of DOX with GelMa in the precursor solution. In the past, injectable GelMa platforms were developed and successfully deployed for the management of conditions such as osteoarthritis. A 2022 review article by Wang *et al*. summarizes the use of various GelMa injectable platforms and the group discusses the various properties that are essential for such delivery systems [37]. In 2020, Suo *et al*. demonstrated the injectability of GelMA hydrogels for cartilage repair, indicating the ability of methacrylate based hydrogels to be injected to the site of action [38]. GelMa is an excipient that heavily contributes to the viscosity of the precursor solution. Presence of hydrochloride salt of DOX may have resulted in certain premature interactions involving GelMa which reduced the overall viscosity of the precursor solution as reported [39]. As for the increase in degree of swelling, it is being hypothesized that the degree of swelling for hydrogels went up upon introduction of a hydrophilic small molecule into its matrix. This can be attributed to the hydrophilic interactions between DOX and polymeric backbone leading to higher levels of water retention [40].

It is indeed true that a higher degree of swelling is attributable to a lower degree of crosslinking. And it is common knowledge that a lower degree of crosslinking may lead to a burst release of DOX. Moreover, DOX HCl being hydrophilic is extremely prone to a burst release. Therefore, a careful balance needs to be maintained between the degree of swelling, which provides certain physical resistance to the efflux of payloads, and degree of crosslinking which provides a chemical resistance. Since DOX loading resulted in a slightly higher degree of swelling which compromised the degree of crosslinking, to curb the burst release, we adopted a strategy to expose the gels to higher duration of UV light. The strategy to increase the degree of crosslinking was previously reported by Martinez *et al*. The study demonstrates the effect of increasing degree of crosslinking to delay the release of therapeutic payload [41]. The study concludes that this release-crosslinking interplay may be attributed to the increased microstructural tortuosity [41].

The mechanism of action for DOX has been widely studied and reported across multiple published literature and a variety of cancer subtypes, including malignant mesothelioma [42–44]. Chaudhari *et al*. have established that increased LDH activity indicated DOX induced cell membrane damage and cytotoxicity [45]. In addition, it is known that DOX induces cell death by free radical formation, ultimately resulting in apoptotic induction via caspase activation, and disruption of mitochondrial membrane potential [46, 47]. Low dose DOX has also been shown to induce a senescence-like phenotype, resembling senescence of normal cells [48]. Moreover, the drug-excipient compatibility data in our study (Fig. 1C and D) indicates no interaction between excipients and DOX, confirming that the released molecule of DOX is identical to free-DOX. Given the well-established mechanism of action for DOX, and DOX-excipient compatibility, authors are confident about the lack of any novel mechanism of cell death following DOX encapsulation in hydrogel formulations.

Intrapleural chemotherapies have been reported in the past with a study from Sugarbaker et. al. being the most promising one. In 2013, the team demonstrated the efficacy of intrapleural intraoperative hyperthermic intervention of cisplatin and this therapy increased the interval for recurrence of MPM to 27.2 months as compared to 12.8 months after conventional chemotherapy [31]. However, this therapeutic intervention was utilized as a post-surgical intervention. The hydrogel system designed in this study potentially may be used as a stand-alone or a combination therapy prior to surgical resection. However, further pre-clinical evaluation is warranted to test this hypothesis. The current study lays solid groundwork to initiate pre-clinical testing. With established CQAs in place, this system can potentially be

injected through a catheter that is used to flush out pleural effusions, circumventing the need for frequent invasive procedures. This type of a system has been developed in the past for post-surgical intervention by Jaiswal *et al*. [49] and this further cement our hypothesis that a local therapy for MPM management will be an effective therapeutic alternative. Moreover, this GelMa-based system can be used as a platform technology with a high degree of tunability in terms of gelling time, release profiles and loading of diverse modalities, making it a potential candidate to be further explored pre-clinically and clinically.

## Conclusion

This one-of-a-kind study demonstrates the ability of GelMa/LAP/BIS hydrogels to delay the release of a hydrophilic small molecule chemotherapeutic, Doxorubicin HCl. Extensive drug-excipient compatibility studies indicated no compatibility issues between DOX and hydrogel components. Moreover, DOX release was sustained over a period of 12 days, indicating a potential for a local therapy in MPM. Multiple reports have indicated the benefits of a local therapy in improving MPM prognosis and developing a hydrogel-based local delivery will aid local delivery while improving patient compliance due to infrequent dosing requirement. Also, use of GelMa as the polymeric backbone promotes cell and tissue binding, while being biocompatible, strengthens the translational aspect of this formulation. This study demonstrates the *in-vitro* utility of DLH and achieved promising results. Having a therapeutic option such as DLH for the treatment and management of MPM would be revolutionary. For hard-to-reach cancers such as MPM, frequent dosing has always been an issue with respect to patient compliance and DLH offers extended therapeutic benefits which potentially will improve treatment acceptance among patients. Moreover, sustained drug delivery systems have been proven to have improved pharmacokinetics, leading to improved efficacy in patients. Our DLH system is capable of prolonging drug release over a couple of weeks and has the tunability to extend the release beyond two weeks. However, pre-clinical studies are necessitated prior to clinical testing to test this hypothesis successfully. Extensive investigation is currently underway to curate a hydrogel-based delivery system for MPM prognosis and we believe this study will serve as base for progressing such platforms through clinics.

**Supplementary Information** The online version contains supplementary material available at https://doi.org/10.1007/s11095-024-03794-z.

**Acknowledgements** This study was supported by research funds provided to VG by College of Pharmacy and Health Sciences (CPHS), St. John's University. NSK was supported by research assistantship provided by an NIH Research Enhancement Award (R15), 1R15HL138606-01A1 to VG. GC was supported by graduate teaching assistantship provided by College of Pharmacy and Health Sciences (CPHS), St. John's University. DGG was supported by private industry funding to VG. The authors would like to acknowledge the Imaging Facility of CUNY Advanced Science Research Center for instrument use, as well as scientific and technical assistance.

**Author Contributions** Nishant S Kulkarni – Conceptualization, Methodology, Validation, Investigation, Execution, Formal analysis, Writing – original draft, Software.
Gautam Chauhan – Methodology, investigation.
Mural Quadros – Methodology, investigation.
Dynandev Gadhave – Methodology, investigation.
Vivek Gupta – Conceptualization, methodology, Writing – review and editing, Supervision, Project administration, Funding acquisition, Resources.

**Data Availability** The data that support the findings of this study are available from the corresponding author, VG, upon reasonable request.

## Declarations

**Competing Interest** The authors declare no conflict of interest.

## References

1. chief-editor. Mesothelioma.com. [cited 2020 Oct 19]. Mesothelioma in the United States | Information by State. Available from: https://www.mesothelioma.com/states/. Accessed Dec 2021.
2. Office of National Statistics. Cancer Survival Rates [Internet]. 2020. Available from: https://www.nuffieldtrust.org.uk/resource/cancer-survival-rates#background. Accessed Dec 2021.
3. Frost G. The latency period of mesothelioma among a cohort of British asbestos workers (1978–2005). Br J Cancer. 2013;109(7):1965–73.
4. Reid A, de Klerk NH, Magnani C, Ferrante D, Berry G, Musk AW, *et al*. Mesothelioma risk after 40 years since first exposure to asbestos: a pooled analysis. Thorax. 2014;69(9):843–50.
5. Mesothelioma.com [Internet]. [cited 2024 Feb 19]. Heather Von St. James. Available from: https://www.mesothelioma.com/about/heather-von-st-james/. Accessed Dec 2021.
6. Brims F. Epidemiology and clinical aspects of malignant pleural mesothelioma. Cancers (Basel). 2021;13(16):4194.
7. Sahu RK, Ruhi S, Jeppu AK, Al-Goshae HA, Syed A, Nagdev S, *et al*. Malignant mesothelioma tumours: molecular pathogenesis, diagnosis, and therapies accompanying clinical studies. Front Oncol. 2023;13:1204722.
8. Landrigan PJ, The WTC. Disaster: Landrigan's Response. Environ Health Perspect. 2004;112(11):A607.
9. Lippmann M, Cohen MD, Chen LC. Health effects of World Trade Center (WTC) Dust: An unprecedented disaster with inadequate risk management. Crit Rev Toxicol. 2015;45(6):492–530.
10. Lee YCG. Surgical resection of mesothelioma: an evidence-free practice. The Lancet. 2014;384(9948):1080–1.

11. Kostron A, Friess M, Crameri O, Inci I, Schneiter D, Hillinger S, *et al*. Relapse pattern and second-line treatment following multimodality treatment for malignant pleural mesothelioma. Eur J Cardiothorac Surg. 2016;49(5):1516–23.
12. Vogelzang NJ, Rusthoven JJ, Symanowski J, Denham C, Kaukel E, Ruffie P, *et al*. Phase III study of pemetrexed in combination with cisplatin versus cisplatin alone in patients with malignant pleural mesothelioma. J Clin Oncol. 2003;21(14):2636–44.
13. Baas P, Scherpereel A, Nowak AK, Fujimoto N, Peters S, Tsao AS, *et al*. First-line nivolumab plus ipilimumab in unresectable malignant pleural mesothelioma (CheckMate 743): a multicentre, randomised, open-label, phase 3 trial. Lancet. 2021;397(10272):375–86.
14. Gautron Moura B, Gerard CL, Testart N, Caikovski M, Wicky A, Aedo-Lopez V, *et al*. Estimated costs of the ipilimumab-nivolumab therapy and related adverse events in metastatic melanoma. Cancers (Basel). 2022;15(1):31.
15. Hyperthermic Intraoperative Intrapleural Chemotherapy, Surgical Cytoreduction As Part Of Multimodal Treatment Of Malignant Pleural Mesothelioma-Case Report, Szkorupa M, Klos D, Chudacek J, Hanuliak J, *et al*. Hyperthermic intraoperative intrapleural chemotherapy and surgical cytoreduction as part of multimodal treatment of malignant pleural mesothelioma - case report M. Szkorupa1, D. Klos1, J. Chudacek1, J. Hanuliak1, M. Stasek1, O. Fischer2, R. Lemstrova3. Rozhl Chir. 2020;99(10):456–61.
16. Li J, Mooney DJ. Designing hydrogels for controlled drug delivery. Nat Rev Mater. 2016;1(12):16071.
17. Zhan J, Wu Y, Wang H, Liu J, Ma Q, Xiao K, *et al*. An injectable hydrogel with pH-sensitive and self-healing properties based on 4armPEGDA and N-carboxyethyl chitosan for local treatment of hepatocellular carcinoma. Int J Biol Macromol. 2020;15(163):1208–22.
18. Fan M, Li M, Wang X, Liao Y, Wang H, Rao J, *et al*. Injectable Thermosensitive Iodine-Loaded Starch-g-poly(N-isopropylacrylamide) Hydrogel for Cancer Photothermal Therapy and Anti-Infection. Macromol Rapid Commun. 2022;43(18):2200203.
19. Melo BL, Lima-Sousa R, Alves CG, Moreira AF, Correia IJ, de Melo-Diogo D. Chitosan-based injectable *in situ* forming hydrogels containing dopamine-reduced graphene oxide and resveratrol for breast cancer chemo-photothermal therapy. Biochem Eng J. 2022;1(185):108529.
20. Lee SY, Jeon SI, Sim SB, Byun Y, Ahn CH. A supramolecular host-guest interaction-mediated injectable hydrogel system with enhanced stability and sustained protein release. Acta Biomater. 2021;1(131):286–301.
21. Vigata M, Meinert C, Pahoff S, Bock N, Hutmacher DW. Gelatin methacryloyl hydrogels control the localized delivery of albumin-bound paclitaxel. Polymers. 2020;12(2):501.
22. Yue K, Trujillo-de Santiago G, Alvarez MM, Tamayol A, Annabi N, Khademhosseini A. Synthesis, properties, and biomedical applications of gelatin methacryloyl (GelMA) hydrogels. Biomaterials. 2015;73:254–71.
23. Xu H, Casillas J, Krishnamoorthy S, Xu C. Effects of Irgacure 2959 and lithium phenyl-2,4,6-trimethylbenzoylphosphinate on cell viability, physical properties, and microstructure in 3D bioprinting of vascular-like constructs. Biomed Mater. 2020;15(5):055021.
24. Wang L, Yang K, Li X, Zhang X, Zhang D, Wang LN, *et al*. A double-crosslinked self-healing antibacterial hydrogel with enhanced mechanical performance for wound treatment. Acta Biomater. 2021;1(124):139–52.
25. Liu Y, Chan-Park MB. A biomimetic hydrogel based on methacrylated dextran-graft-lysine and gelatin for 3D smooth muscle cell culture. Biomaterials. 2010;31(6):1158–70.
26. Hurewitz AN, Zucker S, Mancuso P, Wu CL, Dimassimo B, Lysik RM, *et al*. Human pleural effusions are rich in matrix metalloproteinases. Chest. 1992;102(6):1808–14.
27. Barenholz Y. Doxil®–the first FDA-approved nano-drug: lessons learned. J Control Release. 2012;160(2):117–34.
28. Agrawal K. Doxorubicin. In: xPharm: the comprehensive pharmacology reference [Internet]. Elsevier; 2007 [cited 2021 Nov 15]. pp. 1–5. Available from: https://linkinghub.elsevier.com/retrieve/pii/B9780080552323616502. Accessed Dec 2021.
29. Zidar BL, Pugh RP, Schiffer LM, Raju RN, Vaidya KA, Bloom RL, *et al*. Treatment of six cases of mesothelioma with doxorubicin and cisplatin. Cancer. 1983;52(10):1788–91.
30. Klotz LV, Lindner M, Eichhorn ME, Grützner U, Koch I, Winter H, *et al*. Pleurectomy/decortication and hyperthermic intrathoracic chemoperfusion using cisplatin and doxorubicin for malignant pleural mesothelioma. J Thorac Dis. 2019;11(5):1963–72.
31. Sugarbaker DJ, Gill RR, Yeap BY, Wolf AS, DaSilva MC, Baldini EH, *et al*. Hyperthermic intraoperative pleural cisplatin chemotherapy extends interval to recurrence and survival among low-risk patients with malignant pleural mesothelioma undergoing surgical macroscopic complete resection. J Thorac Cardiovasc Surg. 2013;145(4):955–63.
32. Kulkarni NS, Chauhan G, Goyal M, Sarvepalli S, Gupta V. Development of gelatin methacrylate (GelMa) hydrogels for versatile intracavitary applications. Biomater Sci. 2022;10(16):4492–507.
33. Wong RSH, Dodou K. Effect of drug loading method and drug physicochemical properties on the material and drug release properties of poly (ethylene oxide) hydrogels for transdermal delivery. Polymers (Basel). 2017;9(7):286.
34. Attanoos RL, Churg A, Galateau-Salle F, Gibbs AR, Roggli VL. Malignant mesothelioma and its non-asbestos causes. Arch Pathol Lab Med. 2018;142(6):753–60.
35. Feng Y, Zhang Z, Tang W, Dai Y. Gel/hydrogel-based in situ biomaterial platforms for cancer postoperative treatment and recovery. Exploration (Beijing). 2023;3(5):20220173.
36. Nguyen AK, Goering PL, Reipa V, Narayan RJ. Toxicity and photosensitizing assessment of gelatin methacryloyl-based hydrogels photoinitiated with lithium phenyl-2,4,6-trimethylbenzoylphosphinate in human primary renal proximal tubule epithelial cells. Biointerphases. 2019;14(2):021007.
37. Wang S, Qiu Y, Qu L, Wang Q, Zhou Q. Hydrogels for Treatment of Different Degrees of Osteoarthritis. Frontiers in bioengineering and biotechnology [Internet]. 2022 Jun 6 [cited 2024 Oct 6];10. Available from: https://pubmed.ncbi.nlm.nih.gov/35733529/.
38. Suo H, Li L, Zhang C, Yin J, Xu K, Liu J, *et al*. Glucosamine-grafted methacrylated gelatin hydrogels as potential biomaterials for cartilage repair. J Biomed Mater Res B Appl Biomater. 2020;108(3):990–9.
39. Xuan JJ, Yan YD, Oh DH, Choi YK, Yong CS, Choi HG. Development of thermo-sensitive injectable hydrogel with sustained release of doxorubicin: rheological characterization and in vivo evaluation in rats. Drug Deliv. 2011;18(5):305–11.
40. Nam C, Zimudzi TJ, Geise GM, Hickner MA. Increased hydrogel swelling induced by absorption of small molecules. ACS Appl Mater Interfaces. 2016;8(22):14263–70.
41. Martinez AW, Caves JM, Ravi S, Li W, Chaikof EL. Effects of crosslinking on the mechanical properties, drug release and cytocompatibility of protein polymers. Acta Biomater. 2014;10(1):26–33.
42. Rivankar S. An overview of doxorubicin formulations in cancer therapy. J Cancer Res Ther. 2014;10(4):853.
43 Griffin TW, Stocl M, Collins J, Fernandes J, Maher VE. Combined antitumor therapy with the chemotherapeutic drug doxorubicin

and an anti-transferrin receptor immunotoxin: in vitro and in vivo studies. J Immunother. 1992;11(1):12.
44. Benedetti S, Nuvoli B, Catalani S, Galati R. Reactive oxygen species a double-edged sword for mesothelioma. Oncotarget. 2015;6(19):16848–65.
45. Chaudhari U, Ellis JK, Wagh V, Nemade H, Hescheler J, Keun HC, *et al*. Metabolite signatures of doxorubicin induced toxicity in human induced pluripotent stem cell-derived cardiomyocytes. Amino Acids. 2017;49(12):1955–63.
46. Eom YW, Kim MA, Park SS, Goo MJ, Kwon HJ, Sohn S, *et al*. Two distinct modes of cell death induced by doxorubicin: apoptosis and cell death through mitotic catastrophe accompanied by senescence-like phenotype. Oncogene. 2005;24(30):4765–77.
47. Kciuk M, Gielecińska A, Mujwar S, Kołat D, Kałuzińska-Kołat Ż, Celik I, *et al*. Doxorubicin—an agent with multiple mechanisms of anticancer activity. Cells. 2023;12(4):659.
48. Chang BD, Xuan Y, Broude EV, Zhu H, Schott B, Fang J, *et al*. Role of p53 and p21waf1/cip1 in senescence-like terminal proliferation arrest induced in human tumor cells by chemotherapeutic drugs. Oncogene. 1999;18(34):4808–18.
49. Jaiswal M, Naz F, Dinda AK, Koul V. *In vitro and in vivo* efficacy of doxorubicin loaded biodegradable semi-interpenetrating hydrogel implants of poly (acrylic acid)/gelatin for post surgical tumor treatment. Biomed Mater. 2013;8(4):045004.